Journal of the Geological Society

The Shuilikeng fault in the central Taiwan mountain belt

Giovanni Camanni, Dennis Brown, Joaquina Alvarez-Marron, Yih-Min Wu and Hsi-An Chen

Journal of the Geological Society 2014, v.171; p117-130.
doi: 10.1144/jgs2013-014

Notes

Journal of the Geological Society, London, Vol. **171**, 2014, pp. 117–130. doi: 10.1144/jgs2013-014
Published *Online First* on September 12, 2013

The Shuilikeng fault in the central Taiwan mountain belt

GIOVANNI CAMANNI[1*], DENNIS BROWN[1], JOAQUINA ALVAREZ-MARRON[1], YIH-MIN WU[2] & HSI-AN CHEN[2]

[1]*Institute of Earth Sciences Jaume Almera, ICTJA-CSIC, Lluis Sole i Sabaris s/n, 08028 Barcelona, Spain*
[2]*Department of Geosciences, National Taiwan University, Taipei, 106, Taiwan*
**Corresponding author (e-mail: gcamanni@ictja.csic.es)*

Abstract: For over 200 km along strike the Shuilikeng fault of Taiwan separates Miocene rocks of the Western Foothills from the largely Eocene and Oligocene rocks of the Hsuehshan Range to the east. Despite its importance in the Taiwan mountain belt, the structure and kinematics of the Shuilikeng fault are not well known. Here, we present results from new geological mapping along 100 km of its strike length. At the surface, the Shuilikeng fault is a steeply east-dipping brittle fault with a series of splays and bifurcations. Along its southern part, it cuts an earlier fold and fault system. Outcrop kinematic data vary widely, from thrusting to strike-slip. The surface data are integrated with a relocated and collapsed seismicity database to interpret the fault location at depth. These data indicate that the Shuilikeng fault can be traced to greater than 20 km depth. Some 260 focal mechanisms from this dataset indicate that its kinematics is overall transpressive. From a regional perspective, we interpret the Shuilikeng fault to reactivate a pre-existing rift-related basin-bounding fault to the east of which rocks in the Hsuehshan Range are being exhumed.

The Taiwan mountain belt is often cited as an example *par excellence* of a thin-skinned fold-and-thrust belt (i.e. the sedimentary carapace of the margin is detached above the pre-rift basement) underlain by a shallow detachment that ramps down into the basement only in the easternmost part of the thrust belt (Suppe 1980, 1981, 1987; Tillman & Byrne 1995; Wang *et al.* 2000; Ding *et al.* 2001; Carena *et al.* 2002; Yue *et al.* 2005; Malavieille & Trullenque 2009). Although there is general agreement that this thin-skinned structural model is correct along much of the western part of the orogen, recent studies have suggested that the structure and level of crustal involvement in its internal part may differ significantly from that model (e.g. Wu *et al.* 1997, 2004; Gourley *et al.* 2007; Brown *et al.* 2012). This change takes place across the Shuilikeng fault. Even before it was shown to be a fault, Ichikawa *et al.* (1927) recognized that an important contact existed between what today are known to be Miocene rocks to the west and Eocene–Oligocene rocks to the east. In more recent compilations of Taiwan geology (e.g. Chinese Petroleum Company 1982, 1994; Ho 1988; Chen *et al.* 2000) this contact has been clearly defined as a fault (albeit with different names; see below) that extends from south of Yushan Mountain in central Taiwan to the north coast (Fig. 1). In our study area in central Taiwan (Figs 1 and 2), surface geology (e.g. rock ages, structural style, amount of deformation, level of exhumation), a significant increase in the number and the deeper crustal level of seismic events to the east of the fault and, eastward, higher P-wave velocities at shallower depths, all coincide to indicate a significant change across the Shuilikeng fault (Fig. 1) (Wang *et al.* 2000; Kim *et al.* 2005, 2010; Beyssac *et al.* 2007; Lin 2007; Sakaguchi *et al.* 2007; Simoes *et al.* 2007, 2012; Wu *et al.* 2007; Yamato *et al.* 2009; Brown *et al.* 2012; Kuo-Chen *et al.* 2012). Despite the large amount of data that points toward its importance as a major boundary in the Taiwan orogen, the detailed structure and kinematics of the Shuilikeng fault are not well known. Consequently, it has been interpreted in different ways; for example, as a layer-parallel thrust (the Chukou thrust of Suppe 1981), as a steeply eastward-dipping thrust that extends to deep in the middle crust (the Shuichangliu fault of Wang *et al.* 2002, or the Tulungwan thrust of Rodriguez-Roa & Wiltschko 2010), as a westward-dipping displaced upper part of a pre-existing west-dipping extensional fault (Yue *et al.* 2005), or as a steeply east-dipping transpressional fault that penetrates well into the middle crust (Brown *et al.* 2012). Also, Wiltschko *et al.* (2010) linked it with the Chaochou fault in the south. Neither there is any consensus on whether the Shuilikeng fault is currently active, although recently Sung *et al.* (2000) and Yanites *et al.* (2010) have used river incision, channel morphology and stream gradients along several rivers in central Taiwan to suggest that the Shuilikeng fault has been active throughout the Holocene. By comparing today's stream gradients with those from earlier mapping, Sung *et al.* (2000) furthermore suggested that it has been active during the last 80 years. Nevertheless, even with the large number of earthquakes around it (e.g. Wu *et al.* 2008*a*), seismicity or changes in global positioning system (GPS) velocities are generally not attributed to the Shuilikeng fault (there are exceptions: Yue *et al.* (2005) and Bos *et al.* (2003), respectively), and no surface ruptures have been described from it.

Despite the uncertainties in whether or not the Shuilikeng fault is currently active, there are clear indications from the geological and geophysical data that it is a major structural boundary within the Taiwan mountain belt. Given the wide range of structural interpretations noted above, it is also clear that more detailed studies of the fault are needed to advance our understanding of the structure and kinematics of this orogen. In this paper we present the results of new 1:25000 scale geological mapping and structural analysis along *c.* 100 km (a little less than one-half of its length) of the Shuilikeng fault in central Taiwan (Figs 1 and 2) that further define its map pattern, outcropping structure and kinematics. To help correlate these outcrop data with the location and geometry of the Shuilikeng fault at depth we integrate them with a collapsed seismicity dataset derived from the relocated seismicity database of Wu *et al.* (2008*a*) updated to 2011. Our field kinematic data are augmented by 264 focal mechanism solutions derived from events along the Shuilikeng fault that help place further constraints on its kinematics and recent activity. Finally, we interpret the regional structure and kinematics of the Shuilikeng fault within the context of the Taiwan orogen.

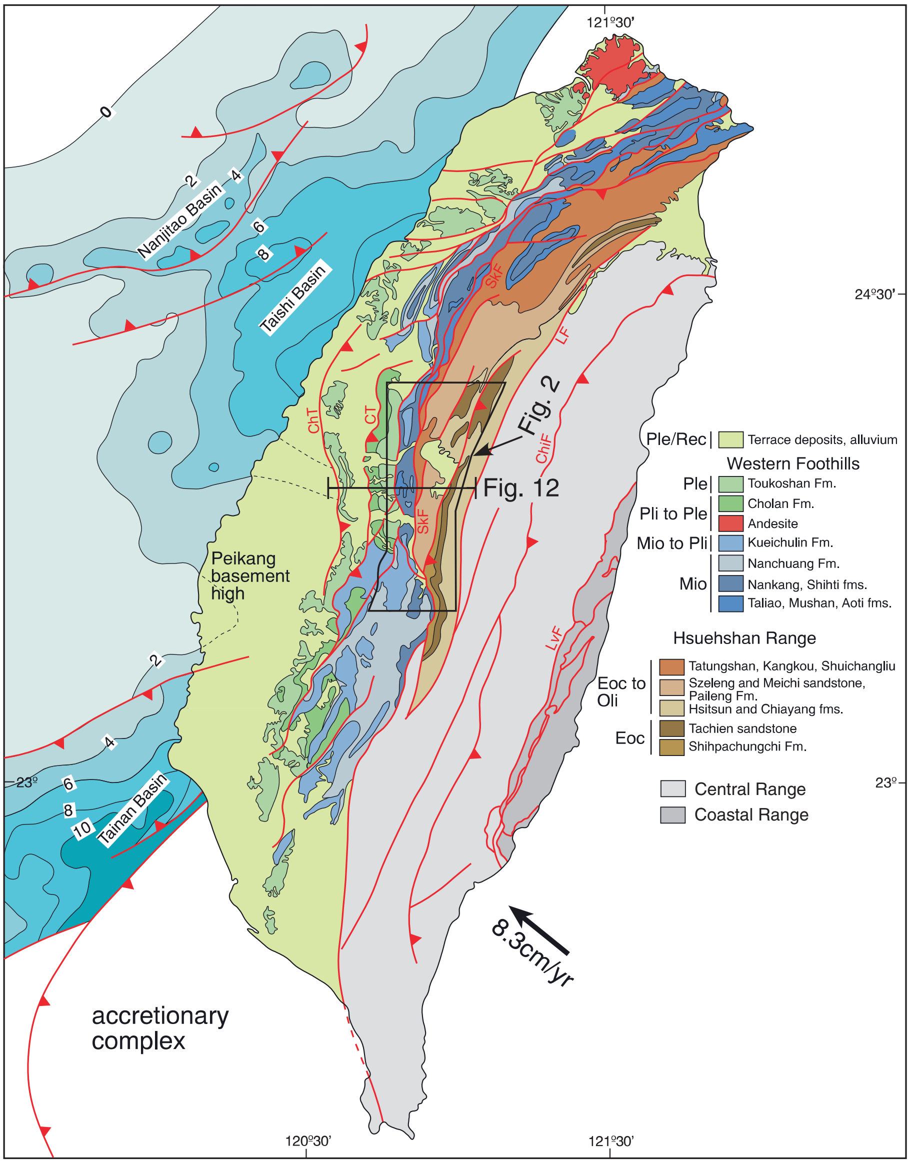

Fig. 1. Simplified geological map of the Taiwan mountain belt (modified after Chen *et al.* 2000). The locations of the study area in Figure 2 and of the crustal cross-section in Figure 12 are shown. Contours offshore indicate the thickness (in km) of the Palaeocene to Miocene sediments in the basins (from Teng & Lin 2004). ChiF, Chinma fault; ChT, Chuanghua thrust; CT, Chelungpu thrust; LF, Lishan fault; LvF, Longitudinal Valley fault; SkF, Shuilikeng fault.

Geological setting

The Taiwan orogen is forming as the result of the latest Miocene to present oblique collision that is taking place between the Luzon arc and the rifted margin of the SE part of Eurasia (Suppe 1984; Huang *et al.* 1997, 2000, 2006; Sibuet & Hsu 2004; Byrne *et al.* 2011). The resultant Taiwan mountain belt is divided into four roughly north–south-oriented tectonostratigraphic zones that are separated by major faults (Fig. 1). From west to east, these zones are the Western Foothills, the Hsuehshan Range, the Central Range and the Coastal Range. The Western Foothills, Hsuehshan Range and Central Range are forming as the result of deformation and uplift of Eocene to Miocene sediments and older pre-rift continental margin rocks of Eurasia and the latest Miocene and younger synorogenic sediments of the foreland basin (e.g. Suppe 1980; Byrne *et al.* 2011; Brown *et al.* 2012). In this paper, we discuss the Western Foothills, which structurally form the frontal part of the mountain belt, and the adjacent Hsuehshan Range. The latter is a more strongly deformed and variably metamorphosed zone to the east (Fig. 1). The focus of this paper is the boundary between these two tectonostratigraphic zones, the Shuilikeng fault. Below we give a brief overview of the outcropping stratigraphy and structure of the Western Foothills and the Hsuehshan Range. Throughout the paper we follow the stratigraphic scheme and nomenclature of Brown *et al.* (2012).

In our study area in central Taiwan (Figs 1 and 2), the Western Foothills are formed by an imbricate thrust system involving latest Miocene to present synorogenic clastic sediments of the foreland basin that, in their easternmost part, are overthrust by Eocene to Miocene unmetamorphosed shallow-water clastic deposits of the Eurasian platform along the Shuangtung thrust (e.g. Suppe 1987; Ho 1988; Yue *et al.* 2005; Castelltort *et al.* 2011; Brown *et al.* 2012; Huang *et al.* 2013). The imbricate thrust system that forms the Western Foothills appears to be linked to a shallow, gently east-dipping detachment developed near the top of the Miocene or at the base of the Pliocene synorogenic sediments (e.g. Suppe 1980, 1981; Ding *et al.* 2001; Carena *et al.* 2002; Yue *et al.* 2005; Brown *et al.* 2012). For an alternative interpretation in which there is extensive basement involvement the reader should see, for example, Mouthereau & Petit (2003), Mouthereau & Lacombe (2006), Simoes *et al.* (2007) and Rodriguez-Roa & Wiltschko (2010). Eastward of the Shuilikeng fault, the Hsuehshan Range is made up

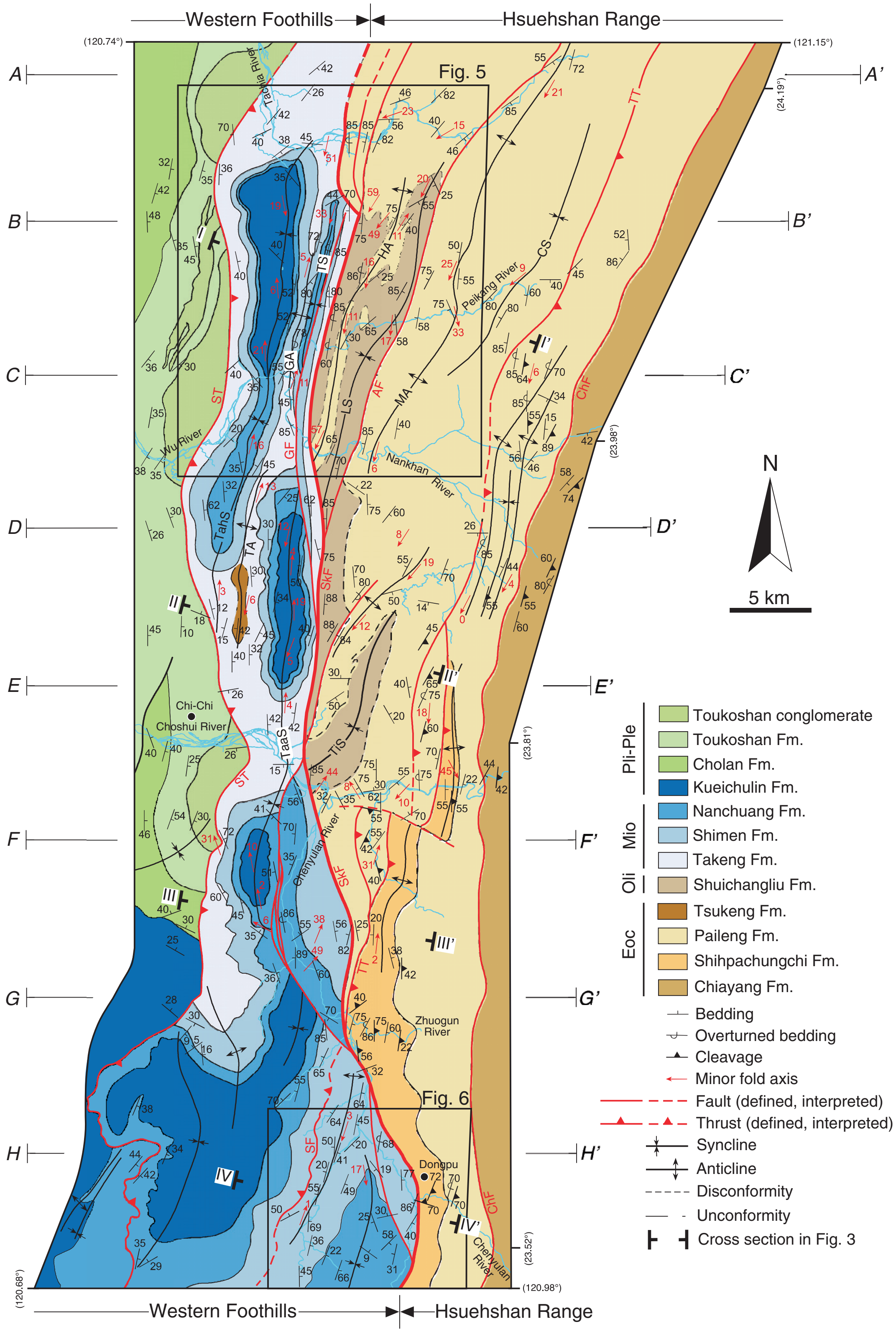

Fig. 2. Geological map of the study area across the Shuilikeng fault in central Taiwan. The location of the map is indicated in Figure 1. The locations of the seismicity sections in Figure 10 (from A–A' to H–H') are shown in black. Fault abbreviations: AF, Alenkeng fault; ChF, Chiayang fault; GF, Guaosing fault; SkF, Shuilikeng fault; SF, Shenmu fault; ST, Shuangtung thrust; TT, Tili thrust. Fold abbreviations: CS, Chuangyuan syncline; GA, Guaosing anticline; HA, Hsiaoan anticline; LS, Lileng syncline; MA, Meitzulin anticline; TA, Tsukeng anticline; TiS, Tingkan syncline; TS, Tachiwei syncline; TaaS, Taanshan syncline; TahS, Tahenpingshan syncline.

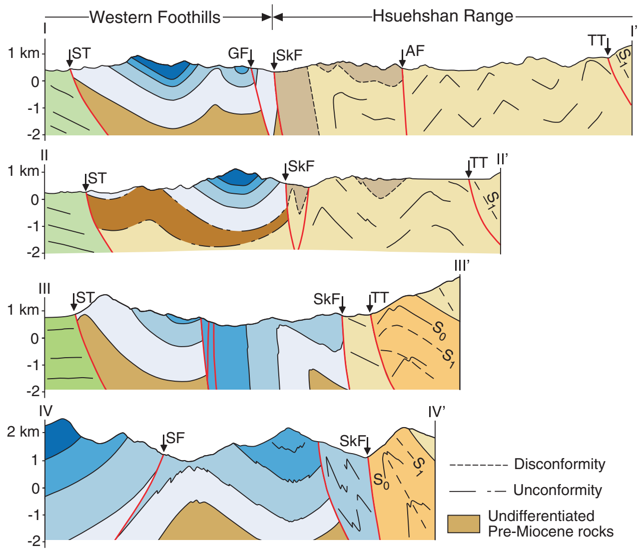

Fig. 3. Geological cross-sections throughout the map area. Their location is indicated in Figure 2. Fault and fold abbreviations, and colours, are as in Figure 2.

of variably metamorphosed Eocene clastic sediments that were deposited in the so-called Hsuehshan Basin during rifting of the Eurasian margin that are disconformably overlain by post-rift Oligocene shale and sandstone (Ho 1988; Huang *et al.* 1997; Lin *et al.* 2003; Teng & Lin 2004). Along much of the western part of the Hsuehshan Range, these rocks are weakly to moderately metamorphosed (Beyssac *et al.* 2007; Simoes *et al.* 2012) and, at least in the central part of the study area, they have been exhumed from between 9.2 and 9.8 km depth (Sakaguchi *et al.* 2007). Eastward and southward, however, in the hanging wall of the Tili thrust (Fig. 2), these rocks reach lower greenschist facies (Clark *et al.* 1993) and have a penetrative pressure solution cleavage (Clark *et al.* 1993; Tillman & Byrne 1995; Fisher *et al.* 2002, 2007; Brown *et al.* 2012).

The Shuilikeng fault at the surface

The Shuilikeng fault crops out poorly along most of its length, limiting direct acquisition of data on its deformation mechanisms, geometry and kinematics. Therefore, the approach taken in this study was to collect field data along and across it to construct the regional map pattern (Fig. 2) and cross-sections (Fig. 3), as well as analyse bedding dips and fold axes (Fig. 4). Where possible, fault orientation and kinematic indicator data were taken (see below). We present local, detailed maps and serial cross-sections from two areas to compare and contrast the differences in structural style along the strike of the fault (Figs 5 and 6).

Regional map pattern

In central Taiwan, a pronounced system of nearly north–south-oriented valleys clearly demarcates the contact between the Miocene rocks of the Western Foothills and the Eocene to Oligocene rocks of the Hsuehshan Range. This contact marks the surface trace of the Shuilikeng fault. The rectilinear map pattern of the fault, in which its trace cuts roughly straight across the

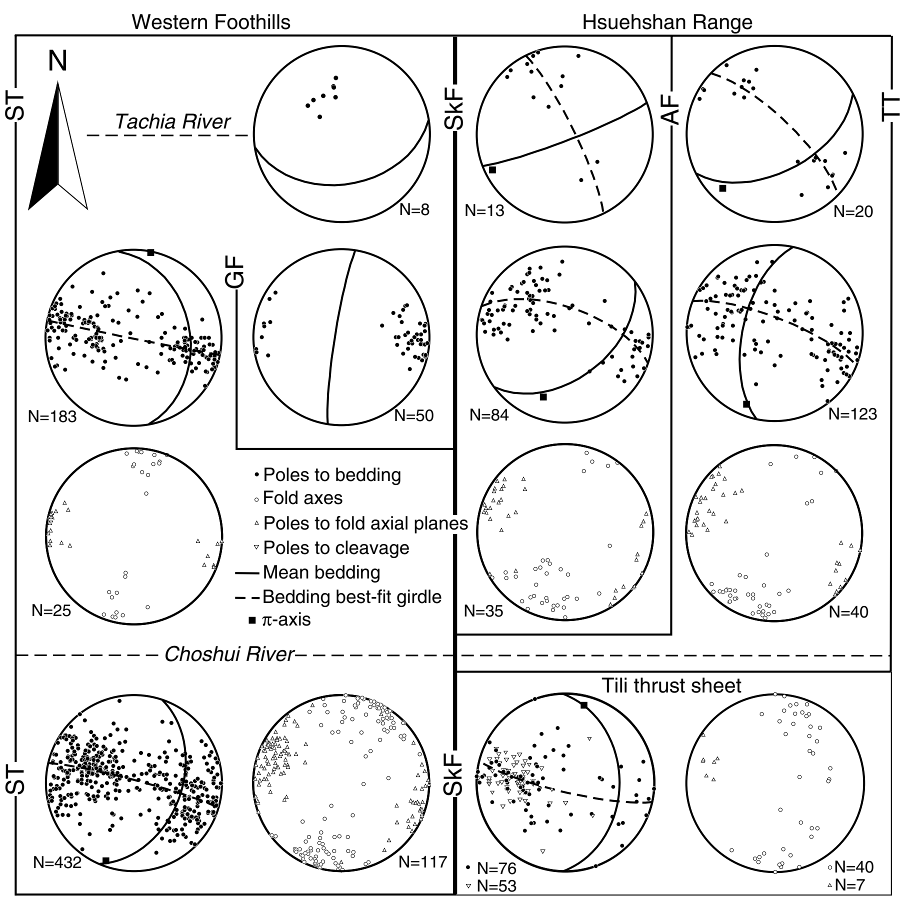

Fig. 4. Stereoplots (lower hemisphere, equal-area projection) of the main structural features within the study area. The grid indicates the subdivision of the map area into sub-areas bounded by the main faults that crop out within the map area. Fault abbreviations are as in Figure 2. The clockwise rotation of all the structural features towards an ENE–WSW orientation along the Tachia River should be noted. Also, the poles to bedding in the area between the Shuilikeng and the Alenkeng faults define two maxima consistent with asymmetric folds (e.g. the Hsiaoan anticline) made up of a steeply NW- to WNW-dipping to overturned forelimb and a moderately SE- to ESE-dipping backlimb.

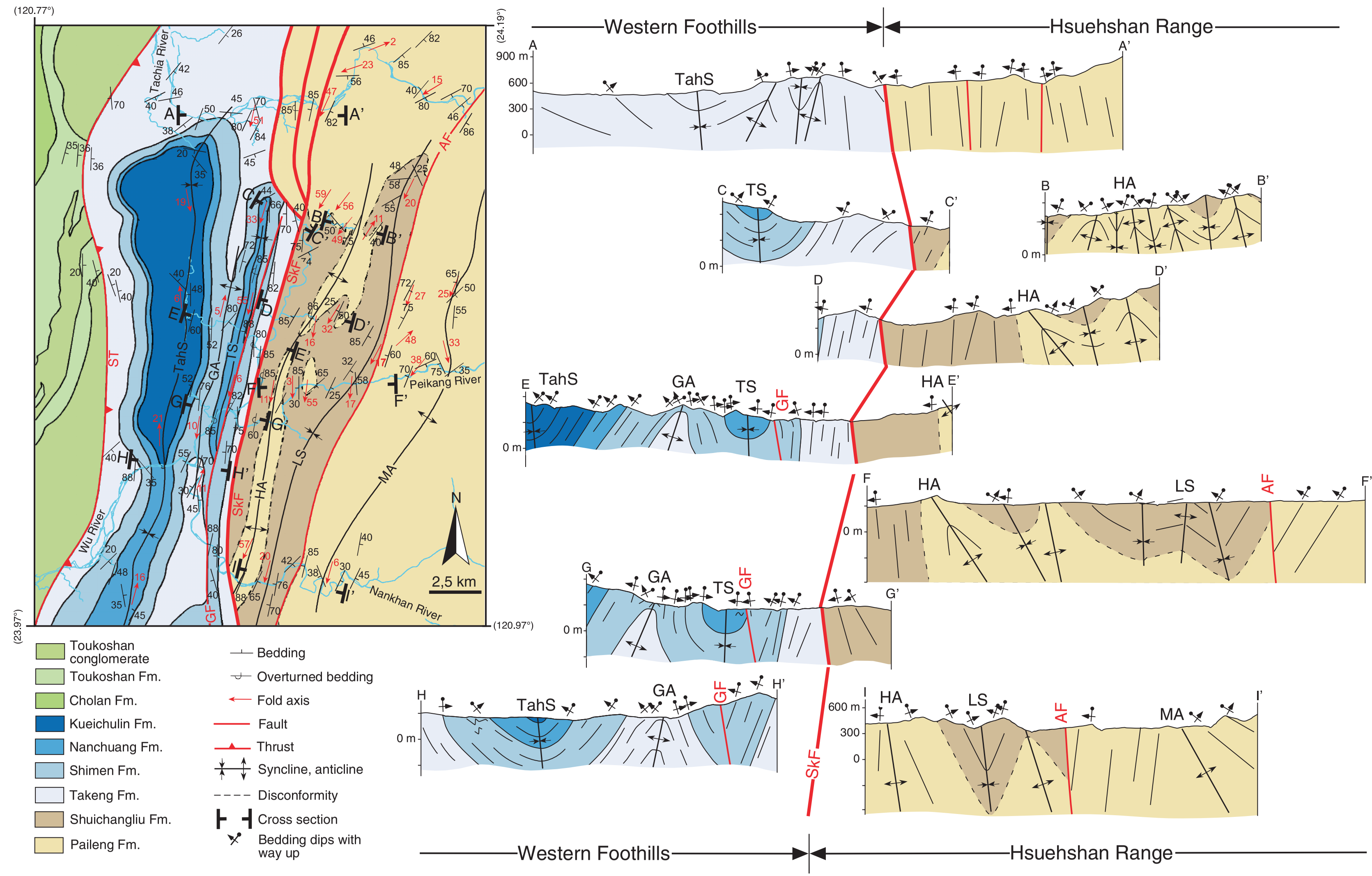

Fig. 5. Detailed geological map and serial cross-sections in the northern part of the map area. The location of the map is indicated in Figure 2. Fault and fold abbreviations are as in Figure 2.

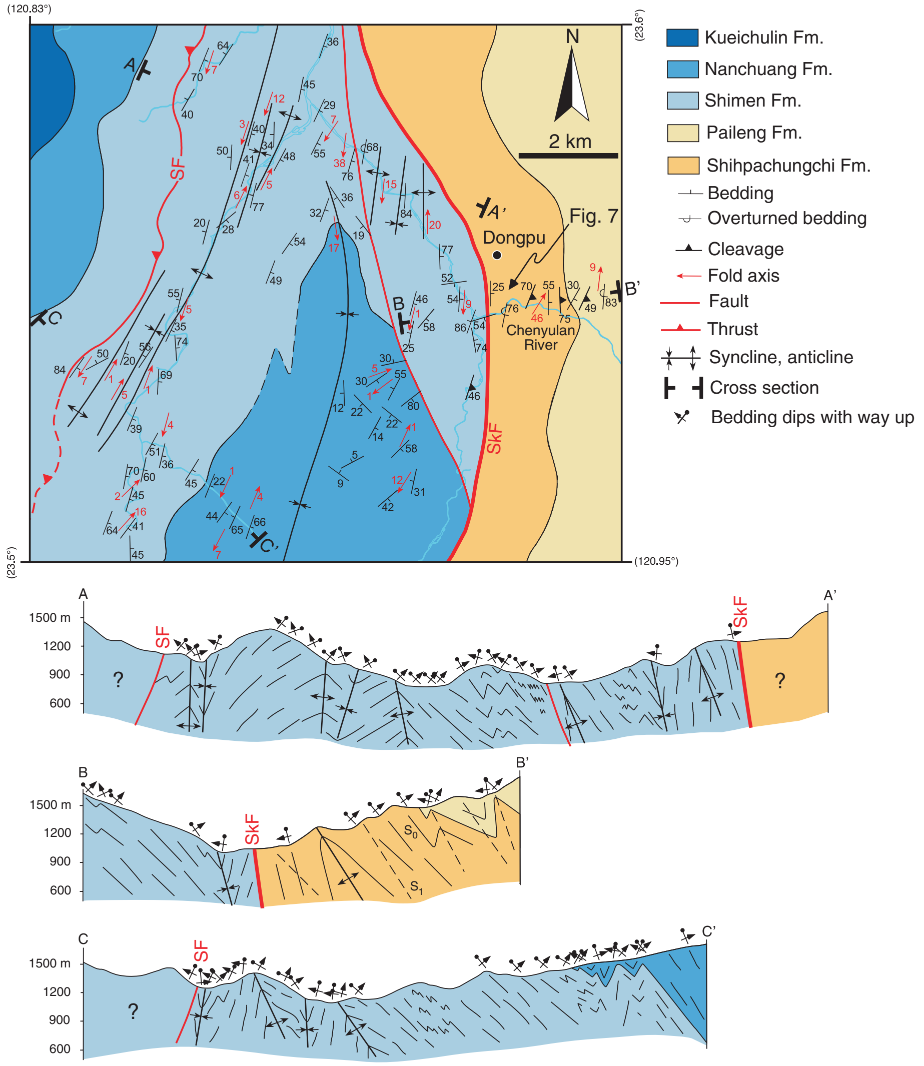

Fig. 6. Detailed geological map and serial cross-sections in the southern part of the map area. The location of the map is indicated in Figure 2. Fault and fold abbreviations are as in Figure 2.

topography, suggests that at the surface it has a steep dip. Within the study area, there are also notable changes from north to south in the map pattern of the fault (Fig. 2). These changes take place across the Choshui River (Figs 2, 3 and 4).

To the north of the Choshui River, the regional structure is that of open, symmetric synclines and anticlines developed west of the Shuilikeng fault and asymmetric slightly west-verging folds to the east (Figs 2 and 3). At a larger scale (Fig. 5), in its hanging wall the Shuilikeng fault juxtaposes weakly metamorphosed Eocene and Oligocene rocks in the west-verging Hsiaoan anticline (HA in Fig. 2) against lower Miocene rocks in open to locally very tight synclines and anticlines in its footwall (see section I–I' in Fig. 3). The Hsiaoan anticline is non-cylindrical, with a vertical to slightly overturned forelimb and with a roughly WSW plunge along the Tachia River and a moderate SW plunge farther south (Fig. 4) where its hinge appears to merge with the Shuilikeng fault (Fig. 5). Folds in the hanging wall of the Shuilikeng fault are cut by several NE–SW-striking faults. For example, the Alenkeng fault cuts the backlimb of the Hsiaoan anticline and places Eocene rocks on top of Oligocene (AF in Figs 2, 3 and 5). In this area, to the west of the Shuilikeng fault, the Tachiwei syncline and Guaosing anticline (TS and GA in Figs 2 and 5) form a gently north- and south-plunging (Fig. 4), tight fold pair that, locally, have a slight east vergence (Fig. 5). The Guaosing fault (GF in Figs 2, 3 and 5) cuts across the eastern limb of the Tachiwei syncline (Fig. 5), suggesting that it either post-dates, or is a late feature in the development of the fold pair. Southward, the southern limb of the Tingkan syncline (TiS in Fig 2) is overturned against the Shuilikeng fault and both limbs are cut by it, suggesting that it predates or records progressive deformation along the fault.

South of the Choshui River, the Shuilikeng fault takes on an anastomosing map pattern in which we can identify two fault-bound lenses of steeply west-dipping to locally overturned Miocene rocks (Figs 2 and 3). In this area, the Tili thrust (TT in Fig. 2) approaches and is cut by the Shuilikeng fault. This is especially apparent along the Zhuogun River (Fig. 2) where the cleavage in the hanging wall of the Tili thrust is folded into an anticline whose forelimb directly abuts the Shuilikeng fault (Fig. 3, section III–III'). Where it abuts the Shuilikeng fault, the rocks in the Tili thrust sheet form a kilometre-scale, tight, west-verging, overall NNE-plunging, anticline with a steep to slightly overturned forelimb and a ESE-dipping axial planar pressure solution cleavage (Fig. 4) (see sections III–III' and IV–IV' in Fig. 3, and section B–B' in Fig. 6). In thin section, we have observed rare, fine-grained biotite replacing chlorite along the cleavage planes, suggesting that these rocks are in greenschist facies, as indicated by Clark *et al.* (1993), Beyssac *et al.* (2007) and Sakaguchi *et al.* (2007). To the west, the Miocene rocks are unmetamorphosed and, adjacent to the fault, the structure is dominated by intense faulting and folding developed on a tens of metres scale

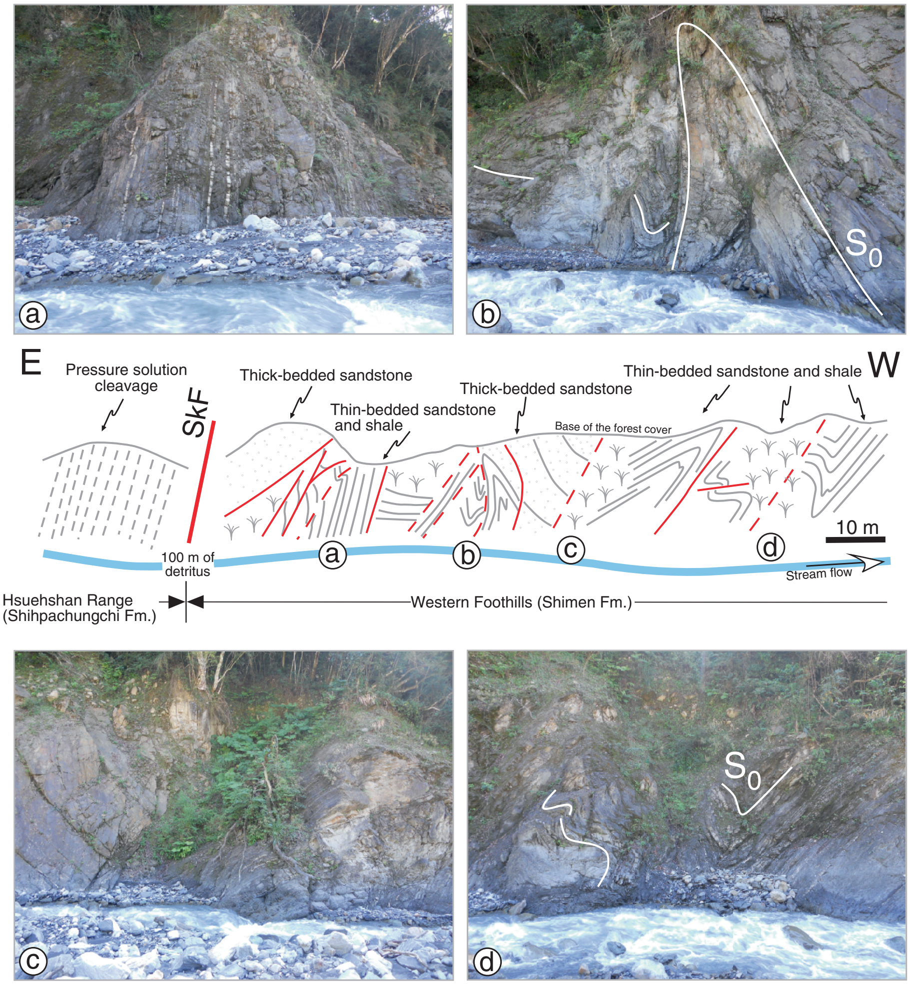

Fig. 7. Sketch and photographs of the high-strain zone developed within the Miocene that defines the Shuilikeng fault in the southernmost part of the map area along the Chenyulan River. The disharmonic folding of the thin-bedded sandstone and shale units and the brecciation of the thick-bedded sandstone units should be noted. The approximate location of the sketch is indicated in Figure 6.

(Fig. 6) that, farther west, becomes a complex interaction of kilometre-scale synclines and anticlines (Fig. 2) that are beyond the scope of this paper. In the area adjacent to the fault, folds are mildly non-cylindrical but with a general shallow NNE–SSW plunge, and are mainly WNW-verging (Figs 4 and 6). A good example of this can be found in the Chenyulan River immediately south of the village of Dongpu (Fig. 6). Here, the Eocene Shihpachungchi Formation can be observed to directly overlie the Middle Miocene Shimen Formation. The Eocene rocks are strongly sheared and tightly folded into a west-verging anticline (Fig. 6, section B–B'). The Miocene rocks in the footwall form a zone of intense brittle faulting and folding of several hundred metres in width (Fig. 7). The majority of the faults are east-dipping and kinematic indicators such as slickenfibres on slip surfaces and small bedding displacements indicate an overall top-to-the-west sense of movement, although we stress that the kinematics is highly variable (see the section on kinematics below). Fold geometries in this area are often very complex, as thick-bedded sandstone units display various degrees of brecciation and boundinage whereas more thin-bedded sandstone and shale units show disharmonic folding (Fig. 7).

Deformation mechanism and kinematics

In the kinematic analysis of fault-slip data, we adopted the approach of Marrett & Allmendinger (1990), which uses the linked Bingham distribution of the shortening and extension directions of a population of faults to calculate the average incremental principal strain axes (i.e. average P and T axes), giving an average fault plane solution.

Where observed in the field, the Shuilikeng fault is everywhere a brittle feature composed of breccia and fault gouge (Fig. 8). Fault and slickenfibre orientation data from a number of locations along the Shuilikeng fault indicate senses of slip that range from thrusting, to strike-slip, to extension. In several localities, slickenfibres developed on slip surfaces, small bedding displacements across discrete faults, and minor fold vergence indicate that all three senses of movement have taken place at different times in the same outcrop. Despite these local complexities, the averaged fault plane solutions indicate a nearly NW–SE to east–west average shortening direction (P axis in Fig. 9) along the length of the Shuilikeng fault. The T axes, however, range from steeply plunging to subhorizontal, resulting in average fault plane solutions for single outcrops that range from thrusting to strike-slip (Fig. 9).

The Shuilikeng fault at depth

Fault location and geometry

On the basis of formation thicknesses, bedding dips, reflection seismic data and standard cross-section construction techniques, Brown *et al.* (2012) have interpreted the location of the Shuilikeng fault at depth in the upper 10 km. For other interpretations in which the Shuilikeng fault (under different names) is interpreted to extend to 10 km and beyond, the reader should see, for example, Wang *et al.*

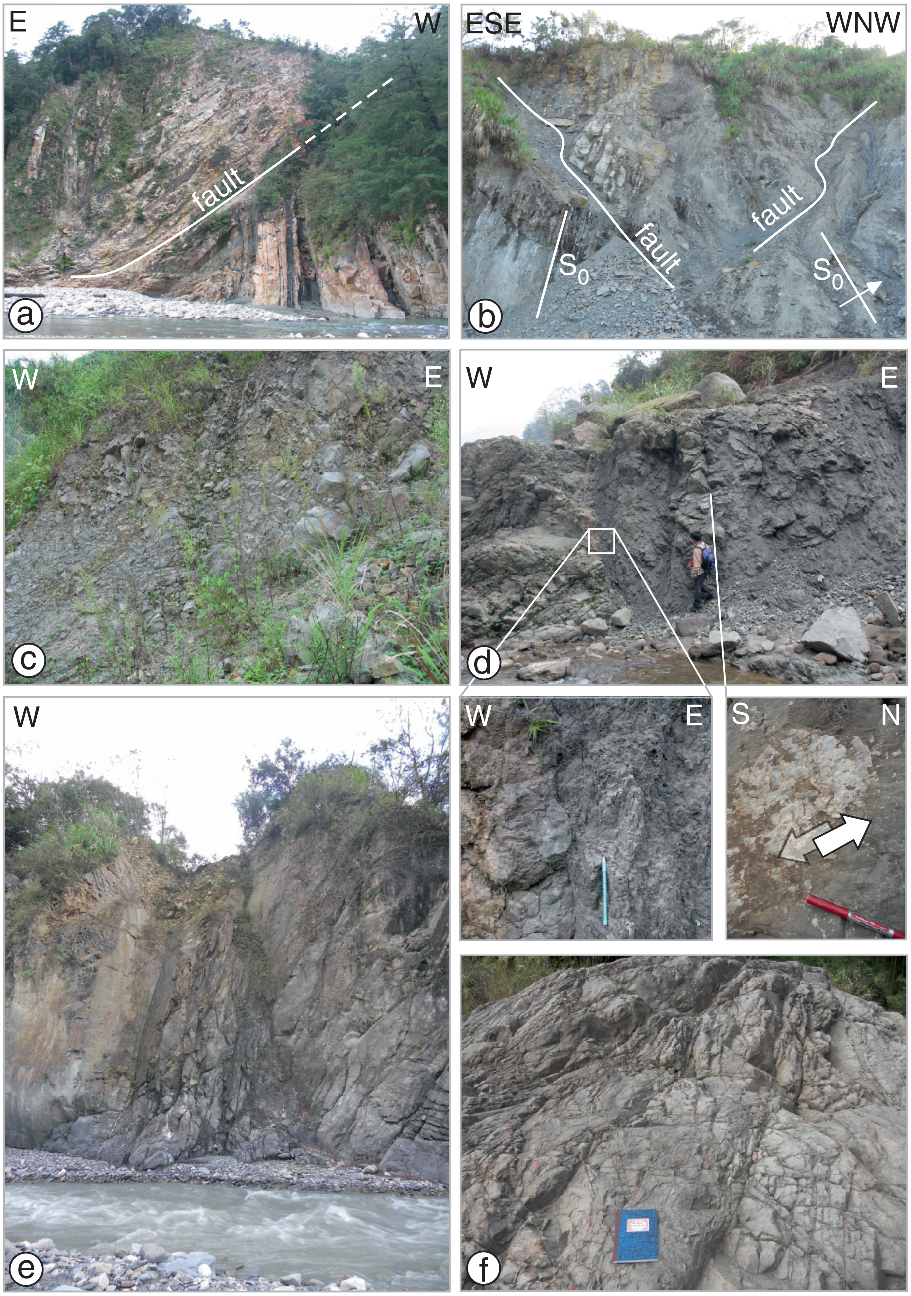

Fig. 8. Field photographs (their location is indicated in Fig. 9). (**a**) Splay of the Shuilikeng fault across the Tachia River in the northernmost part of the map area. (**b, c**) Complex fault zone (**b**) and fault breccia (**c**) that define the Guaosing fault. (**d**) Fault breccia and fault gouge of the Shuilikeng fault immediately south of the Choshui River. (Note slickenfibres on a minor fault surface within this breccia zone indicating a left-lateral strike-slip sense of movement.) (**e, f**) Fault breccia developed within the Shimen Formation that defines the Shuilikeng fault in the southernmost part of the map area, around Dongpu.

(2000) and Rodriguez-Roa & Wiltschko (2010). Here, to interpret the location and geometry of the Shuilikeng fault below 10 km depth, we use the relocated seismicity database of Wu *et al.* (2008*a*; updated to 2011 in our study area) which contains events that range up to >7 M_L. In this paper, these data have been further processed using the collapsing technique of Jones & Stewart (1997), which involves the determination of statistical measurements for standard errors in the depth, latitude and longitude for each event and the clustering of events with overlapping error spheroids. These collapsed data were then plotted in a 3D volume and parallel vertical sections were cut 10 km apart (Figs 2 and 10). Events were projected onto the sections from 4.99 km on either side to avoid having the same event on any two sections. The sections are confined to the upper 20 km of crust to avoid any interference with earthquakes that could be related to the Lishan fault (the structural boundary between the Hsuehshan Range and the Central Range; see, e.g. Lee *et al.* 1997).

The pattern of seismicity in the cross-sections varies significantly from north to south across the study area (Fig. 10). In the northernmost part (sections A–A' and B–B'), the seismic events form a cloud from which we are unable to discriminate any fault zone. In the central part of the map area (sections C–C', D–D', E–E' and F–F'), however, there is a roughly horizontal open cluster of events at 10 km depth (detachment in Fig. 10) that nearly coincides with the location of the basal detachment beneath the Western Foothills (Carena *et al.* 2002; Yue *et al.* 2005; Brown *et al.* 2012). At *c.* km 20, between *c.* 10 and 20 km depth, there is a large, tight cluster of hypocentres that dips *c.* 45–50° eastward (SkF in Fig. 10). This east-dipping cluster of seismicity extends downward from the deep trace of the Shuilikeng fault defined in cross-section by Rodriguez-Roa & Wiltschko (2010) and Brown *et al.* (2012), or along its deep trace as defined by Wang *et al.* (2000). We therefore interpret

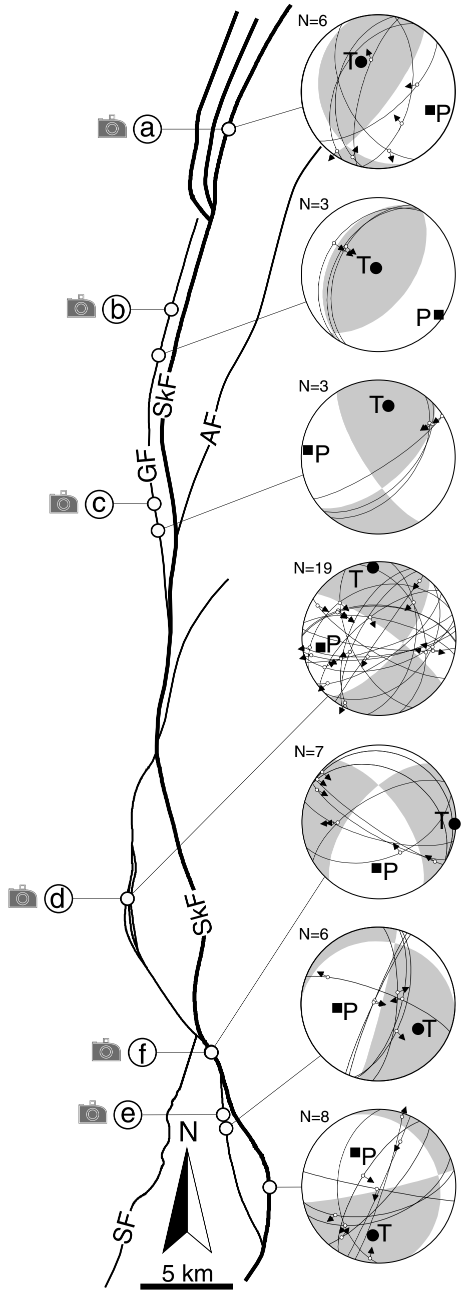

Fig. 9. Fault-slip data (lower hemisphere, equal-area projection) from the Shuilikeng and Guaosing faults. The average P and T axes determined using these data are shown, as are the average fault plane solutions. Fault planes are represented as great circles and the arrows indicate the sense of movement of the hanging-wall block of the faults. The lowercase letters indicate the location of the photographs in Figure 8.

the Shuilikeng fault to link with this cluster of events and to extend to at least 20 km depth. The extensive cloud of seismicity to the east of the surface location of the Shuilikeng fault and above its interpreted subsurface location, especially in sections C–C' and D–D', could possibly be related to the faults in the hanging wall of the Shuilikeng fault discussed above. Southward, in sections G–G' and H–H', the trace of the Shuilikeng fault is less clearly defined from the seismicity pattern, although it can still be interpreted to dip moderately eastward (Fig. 10).

Fault kinematics: earthquake focal mechanisms

To gain insight into the kinematics of the Shuilikeng fault at depth we have used the database of earthquake focal mechanisms of Wu *et al.* (2008*b*, 2010), updated to 2011 in our map area (Fig. 11). The 264 events presented in Figure 11 have been relocated using the 3D velocity model of Wu *et al.* (2007, 2009) and then have been collapsed using the method described in the previous section. In our analysis, the map area has been divided into three zones whose north–south extent were determined to coincide with the beginning of a clear east-dipping band of seismicity in the vertical sections (i.e. between sections B–B' and C–C', and F–F' and G–G'), and east–west to include what we interpret to be the extent of the Shuilikeng fault and the faults in its hanging wall at the surface (Fig. 11). These zones were then divided into four 5 km thick bins, to a depth of 20 km. The fault types (i.e. strike-slip, thrust, normal and other) derived from the focal mechanisms were calculated using the technique of Zoback (1992), which takes into account the plunge of the P, B and T axes of each fault plane solution. To provide further information for the interpretation of the kinematics, all events within each 5 km thick bin were grouped together and the average principal strain axes were calculated using the method of Marrett & Allmendinger (1990) (Fig. 11). For the sake of brevity, below we describe only the average fault plane solutions.

In the northern part of the study area (area 'a' in Fig. 11), there are no data in the upper 5 km. In the bin from 5 to 10 km depth, the average P and T axes are roughly subhorizontal and trend NNW–SSE and ENE–WSW, respectively, resulting in a strike-slip average fault plane solution. From 10 to 20 km depth, however, their trend changes, with the P axis remaining horizontal and trending NW–SE and the T axis becoming nearly vertical, giving a thrust average fault plane solution. In the central part of the map area (area 'b' in Fig. 11), again, there are no data in the first 5 km. In all three bins from 5 to 20 km depth, the average P axis is nearly horizontal and trend NW–SE, whereas the average T axis is vertical, giving a thrust average fault plane solution at all depths. Finally, in the southern part of the map area (area 'c' in Fig. 11), in the bin from 0 to 5 km depth, the average P and T axes are roughly subhorizontal and trend WNW–ESE and NNE–SSW, respectively, giving a strike-slip average fault plane solution. However, from 5 to 15 km depth the T axis becomes vertical, resulting in a thrust average fault plane solution. There are not enough events in the 15–20 km bin to determine statistically meaningful principal strain axes.

Discussion

By combining surface geology and seismicity data, the Shuilikeng fault in central Taiwan can be interpreted to be a brittle fault that dips eastward and reaches more than 20 km depth (Fig. 12). For about 100 km along its strike-length the map pattern defined by the Shuilikeng fault (Fig. 2) is similar to that of other well-known transpressive to strike-slip fault systems (Wilcox *et al.* 1973; Sylvester 1988; Butler *et al.* 1998; Walcott 1998; Nicol & Van Dissen 2002; Kirkpatrick *et al.* 2008; Leever *et al.* 2011; Murphy *et al.* 2011; Dooley & Schreurs 2012). Along its southern end, it cuts an earlier fault and fold system, juxtaposing greenschist-facies rocks in its hanging wall (with a pressure solution cleavage) against unmetamorphosed rocks in its footwall. In the northern part, however, the relationships between the Shuilikeng fault and structures that splay off it are often ambiguous, although from the data given in the previous sections we interpret them to be coeval and linked. The constraints placed on the Shuilikeng fault dip and location in the subsurface by the surface geology (formation thickness and dip,

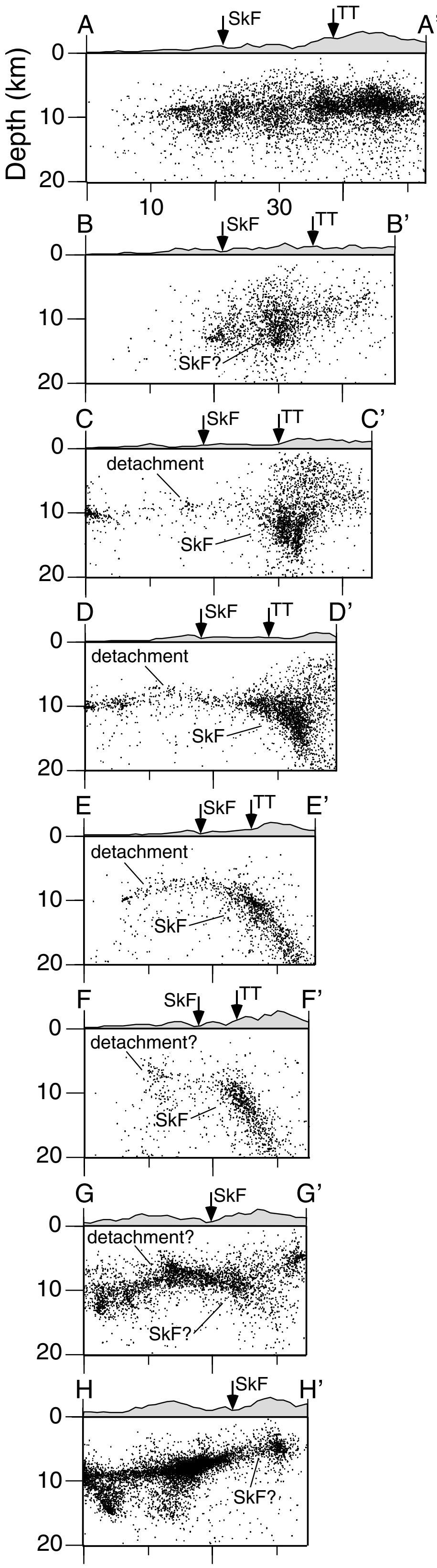

Fig. 10. Seismicity sections through the map area. Seismicity data are projected from 4.99 km on either side of the section. It should be noted how, from section C–C' to section F–F', an east-dipping cluster of seismicity that projects nearly to the location of the Shuilikeng fault at the surface is recognizable. The location of the sections is indicated in Figure 2. SkF, Shuilikeng fault; TT, Tili thrust.

faults, folds etc.) allow it to be extrapolated to a depth of around 10 km (Fig. 12). Although there are uncertainties in this extrapolation, at 10 km depth it coincides with a cluster of east-dipping seismicity that extends to over 20 km depth (Fig. 12). We interpret this seismicity to be related to a steeply dipping fault whose upward trace projects to the Shuilikeng fault at the surface and, we think, is linked to it. Consequently, we interpret the Shuilikeng fault to be an active deep-seated main structure of the Taiwan orogen. Westward, a subhorizontal cluster of seismicity can be interpreted as the detachment to the imbricate stack mapped there, linking it to the thick-skinned deformation east of the Shuilikeng fault (Fig. 12). More work needs to be carried out to determine how this linkage works. Throughout our study area, the kinematics of the Shuilikeng fault is somewhat variable in the surface geological data, whereas the focal mechanism data more consistently indicate NW-directed shortening with strike-slip being active locally in the upper 10 km (Figs 9 and 11). Variability in the surface dataset is possibly the result of successive, overlapping ruptures, whereas variability in the focal mechanism data can, in part, be associated with minor faults. It might also be the result of mechanical decoupling between the kinematics of the fault core and that of the regional fault that has generated it, as suggested for other seismogenic faults (e.g. the San Andreas Fault; Chester *et al.* 1993). Both datasets are consistent, however, with the overall kinematics of the roughly north–south-striking Shuilikeng fault as being transpressive, with the hanging wall moving up toward the NW.

The Eocene rocks of the Hsuehshan Range have been interpreted by Teng *et al.* (1991), Huang *et al.* (1997) and Teng & Lin (2004) to be synrift sediments deposited in a graben or half-graben (the Hsuehshan Basin) on the continental margin of Eurasia. Those researchers further interpreted the Oligocene and Miocene rocks to be post-rift sediments deposited on the margin platform. Although there is a general consensus that the eastern bounding fault of the Hsuehshan Basin probably coincided with the current Lishan fault (Lee *et al.* 1997; Huang *et al.* 1997; Lin *et al.* 2003; Teng & Lin 2004; Wiltschko *et al.* 2010), there is little consensus about the location or even the presence of a western bounding fault (for exceptions see Huang *et al.* 1997; Lee *et al.* 1997). However, for just over 200 km the Shuilikeng fault forms a structural boundary between predominantly Miocene rocks to the west and Eocene rocks of the Hsuehshan Basin to the east (in the north, Oligocene to Miocene rocks also appear; Fig. 1). We suggest, therefore, that the Shuilikeng fault, which at least in central Taiwan penetrates to 20 km or more depth (and must, therefore, affect the basement), can be interpreted to be a major structure that formed along the western margin of the Hsuehshan Basin in the Eocene.

It has been shown that such pre-existing structures on a continental margin can play an important role in many aspects of the evolution of an orogen during mountain building (e.g. Wiltschko & Eastman 1983; Hatcher & Williams 1986; Laubscher 1987; Rodgers 1987; Woodward 1988; Schmidt *et al.* 1988; Narr & Suppe 1994; Butler *et al.* 1997; Pérez-Estaún *et al.* 1997; Brown *et al.* 1999). For example, their reactivation may lead to the inversion of pre-existing rift basins and to the uplift of the synrift rocks and their basement (Bonini *et al.* 2012, and references therein). How the shortening in central Taiwan is resolved to form single faults and fault systems is in general complex (e.g. Bos *et al.* 2003; Gourley *et al.* 2007; Mouthereau *et al.* 2009; Wu *et al.* 2010; Ching *et al.* 2011) and, in many cases, conditioned by the presence of pre-collisional rift basins that were present on the Eurasian margin (e.g. Wu *et al.* 1997; Mouthereau *et al.* 2002; Mouthereau & Lacombe 2006; Hwang *et al.* 2007; Byrne *et al.* 2011; Brown *et al.* 2012). Faults bounding the basins around the Peikang Basement High (see Teng *et al.* (1991), Teng & Lin (2004) and Byrne *et al.* (2011) for an overview of this feature) (Fig. 1), with their significant amount of

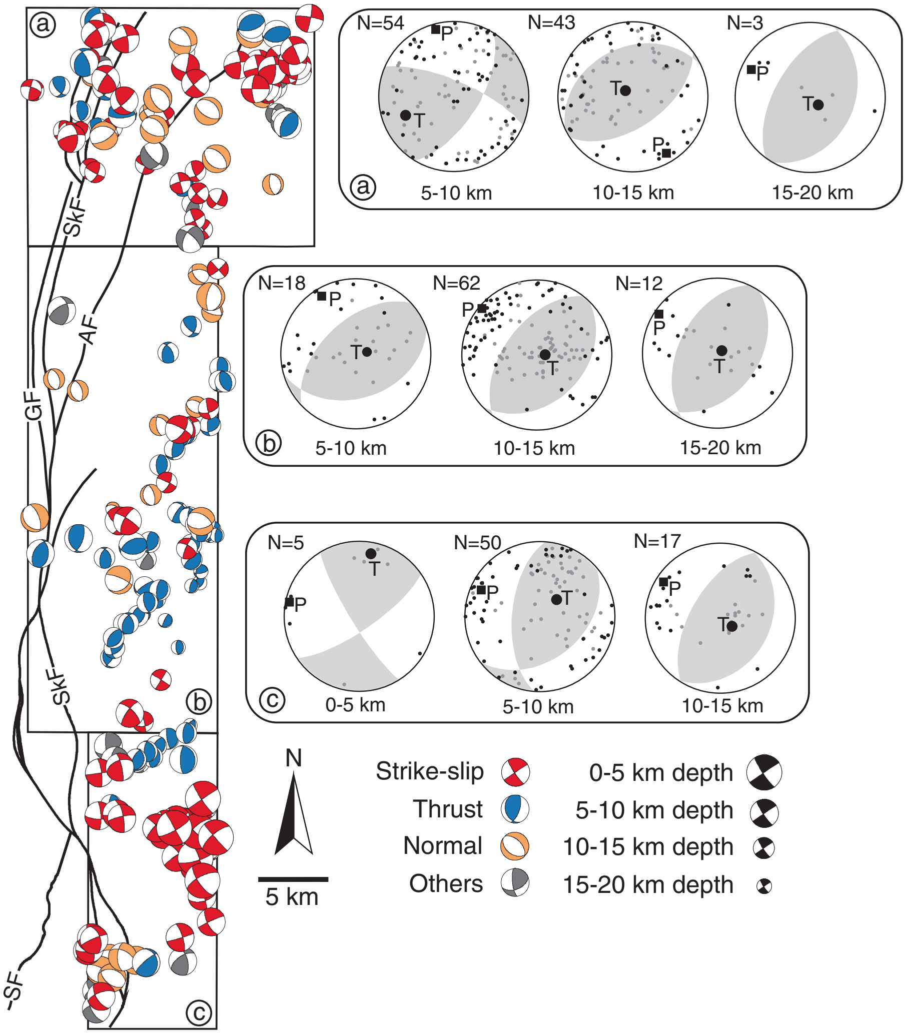

Fig. 11. Earthquake focal mechanisms and variations of the average strain field throughout the map area. The average principal strain axes are calculated from 0 to 20 km depth, at 5 km depth intervals.

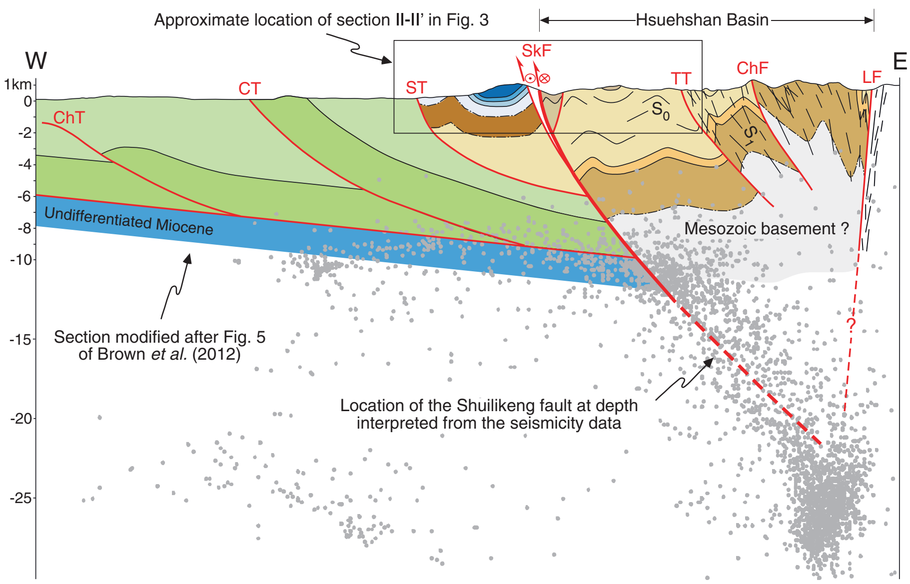

Fig. 12. Crustal cross-section through the central part of the study area (modified after Brown *et al.* 2012). The location is indicated in Figure 1. Seismicity data are projected from 4.99 km on either side of the section. Fault abbreviations are as in Figures 1 and 2, and colours are as in Figure 2.

seismic activity, are an important example of how this mechanism of reactivation of pre-existing basin faults can affect the structural development of the mountain belt (Rau & Wu 1995; Mouthereau *et al.* 2002; Mouthereau & Lacombe 2006; Wu *et al.* 2007; Byrne *et al.* 2011; Chi 2012; Mirakian *et al.* 2012). In central Taiwan, the Shuilikeng fault forms part of this fault system, although how it interacts with many of the other faults around the Peikang Basement High is still not completely understood. Nevertheless, our data suggest that this part of the Shuilkeng fault is currently active and that the western margin of the Hsuehshan Basin is being inverted and exhumed along it. Several researchers have shown that P-wave velocities also increase eastward across the Shuilikeng fault (Kim *et al.* 2005, 2010; Lin 2007; Wu *et al.* 2007; Kuo-Chen *et al.* 2012). If we assume that the Eocene rocks in the Hsuehshan Range are synrift, then the pre-rift Mesozoic basement beneath them should be being exhumed to be within a few kilometres of the surface and these rocks should have higher P-wave velocities. This interpretation is partly corroborated by the thermal data of Sakaguchi *et al.* (2007), who suggested that the Eocene rocks to the east of the Shuilikeng fault have been exhumed from *c.* 10 km depth, which would be in agreement with basement rocks reaching the shallow subsurface in this part of the Hsuehshan Range. This interpretation is also supported by the surface geology (e.g. rock ages, structural style, amount of deformation, level of exhumation), the significant increase in the number and the deeper crustal level of seismic events to the east of the fault and, eastward, higher P-wave velocities at shallower depths (Wang *et al.* 2000; Kim *et al.* 2005, 2010; Beyssac *et al.* 2007; Lin 2007; Sakaguchi *et al.* 2007; Simoes *et al.* 2007, 2012; Wu *et al.* 2007; Yamato *et al.* 2009; Brown *et al.* 2012; Kuo-Chen *et al.* 2012). Based on these data, the regional-scale structure of the Hsuehshan Range in the study area can be interpreted to be a basement-cored anticlinorium (Brown *et al.* 2012; see also Clark *et al.* 1993, for discussion of it as a 'pop-up' structure) (Fig. 12). The highest structural and topographic level that the basement reaches in central Taiwan is over 3000 m above sea level, to the east in the Central Range (see fig. 13 of Brown *et al.* (2012) for a regional interpretation of this structure).

Conclusions

We show that in central Taiwan the Shuilikeng fault is a brittle fault along the western limit of the outcropping Oligocene and Eocene rocks of the Hsuehshan Range. Although kinematic data collected from outcrops along the fault show a degree of variability, when combined with an extensive focal mechanism dataset from within the hypocentre cluster, the overall fault mechanism is clearly transpressive. In its southern part it clearly cuts the Tili thrust and the Tingkan syncline. Northward, however, the relationships between faults and folds splaying off the Shuilikeng fault are not so clear, although they appear to be related to the transpressive deformation taking place in its hanging wall. On the basis of geometrical constraints used for regional cross-section construction (Fig. 12), the surface trace of the Shuilikeng fault can be extrapolated to *c.* 10 km depth where, in the central part of our study area, it coincides with an east-dipping cluster of seismicity. We interpret this cluster of earthquake hypocentres to project from greater than 20 km depth, upward along the Shuilikeng fault to its location at the surface. As a consequence we interpret the fault to be active. This hypocentre cluster may link with a subhorizontal cluster to the west, beneath the imbricate stack of the Western Foothills, but our data provide no clues as to how this entire system works kinematically or mechanically. More work needs to be carried out to clarify this. In a regional context, the Shuilikeng fault can be interpreted to be reactivating a pre-existing fault that was along the western boundary of the Hsuehshan Basin, inverting the basin and causing uplift and exhumation of the Eocene synrift rocks and most probably its underlying basement.

We would like to thank L.-Y. Chao for providing the code for calculating the collapsed seismicity dataset presented in this paper. T. Byrne and an anonymous reviewer are thanked for their constructive comments on the paper. This research was carried out with the aid of grants by CSIC—Proyectos Intramurales 2006 301010, and CGL2009-11843-BTE, and JAE-Predoc.

References

Beyssac, O., Simoes, M., Avouac, J.P., Farley, K.A., Chen, Y.-G., Chan, Y.-C. & Goffé, B. 2007. Late Cenozoic metamorphic evolution and exhumation of Taiwan. *Tectonics*, **26**, http://dx.doi.org/10.1029/2006TC002064.

Bonini, M., Sani, F. & Antonielli, B. 2012. Basin inversion and contractional reactivation of inherited normal faults: A review based on previous and new experimental models. *Tectonophysics*, **522–523**, 55–88, http://dx.doi.org/10.1016/j.tecto.2011.11.014.

Bos, A.G., Spakman, W. & Nyst, M.C.J. 2003. Surface deformation and tectonic setting of Taiwan inferred from a GPS velocity field. *Journal of Geophysical Research*, **108**, http://dx.doi.org/10.1029/2002JB002336.

Brown, D., Alvarez-Marron, J., Perez-Estaun, A., Puchkov, V. & Ayala, C. 1999. Basement influence on foreland thrust and fold belt development: An example from the southern Urals. *Tectonophysics*, **308**, 459–472, http://dx.doi.org/10.1016/S0040-1951(99)00147-X.

Brown, D., Alvarez-Marron, J., Schimmel, M., Wu, Y.M. & Camanni, G. 2012. The structure and kinematics of the central Taiwan mountain belt derived from geological and seismicity data. *Tectonics*, **31**, http://dx.doi.org/10.1029/2012TC003156.

Butler, R.W.H., Holdsworth, R.E. & Lloyd, G.E. 1997. The role of basement reactivation in continental deformation. *Journal of the Geological Society, London*, **154**, 69–71, http://dx.doi.org/10.1144/gsjgs.154.1.0069.

Butler, R.W.H., Spencer, S. & Griffiths, H.M. 1998. The structural response to evolving plate kinematics during transpression: evolution of the Lebanese restraining bend of the Dead Sea Transform. *In:* Holdsworth, R.E., Strachan, R.A. & Dewey, J.F. (eds) *Continental Transpressional and Transtensional Tectonics*. Geological Society, London, Special Publications, **135**, 81–106, http://dx.doi.org/10.1144/GSL.SP.1998.135.01.06.

Byrne, T., Chan, Y.C., Rau, R.J., Lu, C.Y., Lee, Y.H. & Wang, Y.J. 2011. The arc–continent collision in Taiwan. *In*: Brown, D. & Ryan, P.D. (eds) *Arc–Continent Collision*. Springer, Berlin, 213–245.

Carena, S., Suppe, J. & Kao, H. 2002. Active detachment of Taiwan illuminated by small earthquakes and its control of first-order topography. *Geology*, **30**, 935–938, http://dx.doi.org/10.1130/0091-7613(2002)0302.0.CO;2.

Castelltort, S., Nagel, S., *et al.* 2011. Sedimentology of early Pliocene sandstones in the south-western Taiwan foreland: Implications for basin physiography in the early stages of collision. *Journal of Asian Earth Sciences*, **40**, 52–71, http://dx.doi.org/10.1016/j.jseaes.2010.09.005.

Chen, C.-H., Ho, H.-C., *et al.* 2000. *Geological Map of Taiwan. 1:500,000 scale*. Central Geological Survey, Taipei.

Chester, F.M., Evans, J.P. & Biegel, R.L. 1993. Internal structure and weakening mechanisms of the San Andreas Fault. *Journal of Geophysical Research*, **98**, 771–786, http://dx.doi.org/10.1029/92JB01866.

Chi, W.-C. 2012. Coseismic indentor-related deformation during the termination of subduction and its associated geophysical characteristics: an example from Taiwan. *Lithosphere*, **4**, 594–602, http://dx.doi.org/10.1130/L193.1.

Chinese Petroleum Company 1982. *Geological map No. 4. Taichung, 1:100,000*. Taiwan Petroleum Exploration Division, Chinese Petroleum Company, Taipei.

Chinese Petroleum Company 1994. *Geological map No. 3. Miaoli, 1:100,000*. Taiwan Petroleum Exploration Division, Chinese Petroleum Company, Taipei.

Ching, K.-E., Rau, R.-J., Johnson, K.M., Lee, J.-C. & Hu, J.-C. 2011. Present-day kinematics of active mountain building in Taiwan from GPS observations during 1995–2005. *Journal of Geophysical Research*, **116**, http://dx.doi.org/10.1029/2010JB008058.

Clark, M.B., Fisher, D.M., Lu, C.-Y. & Chen, C.-H. 1993. Kinematic analyses of the Hsüehshan Range, Taiwan: a large-scale pop-up structure. *Tectonics*, **12**, 205–217, http://dx.doi.org/10.1029/92TC01711.

Ding, Z.Y., Yang, Y.Q., Yao, Z.X. & Zhang, G.H. 2001. A thin-skinned collisional model for the Taiwan orogeny. *Tectonophysics*, **332**, 321–331, http://dx.doi.org/10.1016/S0040-1951(00)00289-4.

Dooley, T.P. & Schreurs, G. 2012. Analogue modelling of intraplate strike-slip tectonics: A review and new experimental results. *Tectonophysics*, **574–575**, 1–71, http://dx.doi.org/10.1016/j.tecto.2012.05.030.

Fisher, D.M., Lu, C.-Y. & Chu, H.-T. 2002. Taiwan slate belt: Insights into the ductile interior of an arc–continent collision. *In*: Byrne, T. & Liu, C.S. (eds) *Geology and Geophysics of an Arc–Continent Collision, Taiwan*.

Geological Society of America, Special Papers, **358**, 93–106, http://dx.doi.org/10.1130/0-8137-2358-2.9.

Fisher, D.M., Willett, S., Yeh, E.-C. & Clark, M.B. 2007. Cleavage fronts and fans as reflections of orogen stress and kinematics in Taiwan. *Geology*, **35**, 65–68, http://dx.doi.org/10.1130/G22850A.1.

Gourley, J.R., Byrne, T., Chan, Y.-C., Wu, F. & Rau, R.-J. 2007. Fault geometries illuminated from seismicity in central Taiwan: implications for crustal scale structural boundaries in the northern Central Range. *Tectonophysics*, **445**, 168–185, http://dx.doi.org/10.1016/j.tecto.2007.08.013.

Hatcher, R.D. & Williams, R.T. 1986. Mechanical model for single thrust sheets Part I: Taxonomy of crystalline thrust sheets and their relationships to the mechanical behavior of orogenic belts. *Geological Society of America Bulletin*, **97**, 975–985, http://dx.doi.org/10.1130/0016-7606(1986)972.

Ho, C.-S. 1988. *An introduction to the geology of Taiwan: Explanatory text of the geological map of Taiwan*. Central Geological Survey, Taipei.

Huang, C.-Y., Wu, W.-Y., Chang, C.-P., Tsao, S., Yuan, P.B., Lin, C.-W. & Xia, K.-Y. 1997. Tectonic evolution of accretionary prism in the arc–continent collision terrane of Taiwan. *Tectonophysics*, **281**, 31–51, http://dx.doi.org/10.1016/S0040-1951(97)00157-1.

Huang, C.-Y., Yuan, P.B., Lin, C.-W., Wang, T.K. & Chang, C.-P. 2000. Geodynamic processes of Taiwan arc–continent collision and comparison with analogs in Timor, Papua New Guinea, Urals and Corsica. *Tectonophysics*, **325**, 1–21, http://dx.doi.org/10.1016/S0040-1951(00)00128-1.

Huang, C.-Y., Yuan, P.B. & Tsao, S.J. 2006. Temporal and spatial records of active arc–continent collision in Taiwan: A synthesis. *Geological Society of America Bulletin*, **118**, 274–288, http://dx.doi.org/10.1130/B25527.1.

Huang, C.-Y., Chi, W.-R., *et al.* 2013. The first record of Eocene tuff in a Paleogene rift basin near Nantou, Western Foothills, central Taiwan. *Journal of Asian Earth Sciences*, **69**, 3–16, http://dx.doi.org/10.1016/j.jseaes.2013.02.022.

Hwang, C., Hsiao, Y.-S., Shih, H.-C., Yang, M., Chen, K.-H., Forsberg, R. & Olesen, A.V. 2007. Geodetic and geophysical results from a Taiwan airborne gravity survey: Data reduction and accuracy assessment. *Journal of Geophysical Research*, **112**, http://dx.doi.org/10.1029/2005JB004220.

Ichikawa, Y., Honma, U., Haruta, M., Hamaoto, K., Ichihara, H. & Suzuki, T. 1927. *Geological Map of Taiwan*. Government-General of Taiwan, Taipei.

Jones, R.H. & Stewart, R.C. 1997. A method for determining significant structures in a cloud of earthquakes. *Journal of Geophysical Research*, **102**, 8245–8254, http://dx.doi.org/10.1029/96JB03739.

Kim, K.-H., Chiu, J.-M., Pujol, J., Chen, K.-C., Huang, B.-S., Yeh, Y.-H. & Shen, P. 2005. Three-dimensional VP and VS structural models associated with the active subduction and collision tectonics in the Taiwan region. *Geophysical Journal International*, **162**, 204–220, http://dx.doi.org/10.1111/j.1365-246X.2005.02657.x.

Kim, K.-H., Chen, K.-C., Wang, J.-H. & Chiu, J.-M. 2010. Seismogenic structures of the 1999 Mw 7.6 Chi-Chi, Taiwan, earthquake and its aftershocks. *Tectonophysics*, **489**, 119–127, http://dx.doi.org/10.1016/j.tecto.2010.04.011.

Kirkpatrick, J.D., Shipton, Z.K., Evans, J.P., Micklethwaite, S., Lim, S.J. & McKillop, P. 2008. Strike-slip fault terminations at seismogenic depths: The structure and kinematics of the Glacier Lakes fault, Sierra Nevada, United States. *Journal of Geophysical Research*, **113**, http://dx.doi.org/10.1029/2007JB005311.

Kuo-Chen, H., Wu, F.T. & Roecker, S.W. 2012. Three-dimensional P velocity structures of the lithosphere beneath Taiwan from the analysis of TAIGER and related seismic data sets. *Journal of Geophysical Research*, **117**, http://dx.doi.org/10.1029/2011JB009108.

Laubscher, H.P. 1987. Die tektonische Entwicklung der Nordschweiz. *Eclogae Geologicae Helvetiae*, **80**, 287–303.

Lee, J.-C., Angelier, J. & Chu, H.-T. 1997. Polyphase history of a complex major fault zone in the northern Taiwan mountain belt: The Lishan Fault. *Tectonophysics*, **274**, 97–115, http://dx.doi.org/10.1016/S0040-1951(96)00300-9.

Leever, K.A., Gabrielsen, R.H., Faleide, J.I. & Braathen, A. 2011. A transpressional origin for the West Spitsbergen fold-and-thrust belt: Insight from analog modeling. *Tectonics*, **30**, http://dx.doi.org/10.1029/2010TC002753.

Lin, C.-H. 2007. Tomographic image of crustal structures across the Chelungpu fault: Is the seismogenic layer structure- or depth-dependent? *Tectonophysics*, **443**, 271–279, http://dx.doi.org/10.1016/j.tecto.2007.01.022.

Lin, A.T., Watts, A.B. & Hesselbo, S.P. 2003. Cenozoic stratigraphy and subsidence history of the South China Sea margin in the Taiwan region. *Basin Research*, **15**, 453–478, http://dx.doi.org/10.1046/j.1365-2117.2003.00215.x.

Malavieille, J. & Trullenque, G. 2009. Consequences of continental subduction on forearc basin and accretionary wedge deformation in SE Taiwan: Insights from analogue modeling. *Tectonophysics*, **466**, 377–394, http://dx.doi.org/10.1016/j.tecto.2007.11.016.

Marrett, R. & Allmendinger, R.W. 1990. Kinematic analysis of fault-slip data. *Journal of Structural Geology*, **12**, 973–986, http://dx.doi.org/10.1016/0191-8141(90)90093-E.

Mirakian, D.C., Crespi, J.M., Byrne, T.B., Huang, C., Ouimet, W.B. & Lewis, J.C. 2012. Tectonic implications of nonparallel topographic and structural curvature in the higher elevations of an active collision zone, Taiwan. *Lithosphere*, http://dx.doi.org/10.1130/L232.1.

Mouthereau, F. & Lacombe, O. 2006. Inversion of the Paleogene Chinese continental margin and thick-skinned deformation in the Western Foreland of Taiwan. *Journal of Structural Geology*, **28**, 1977–1993, http://dx.doi.org/10.1016/j.jsg.2006.08.007.

Mouthereau, F. & Petit, C. 2003. Rheology and strength of the Eurasian continental lithosphere in the foreland of the Taiwan collision belt: Constraints from seismicity, flexure, and structural styles. *Journal of Geophysical Research*, **108**, http://dx.doi.org/10.1029/2002JB002098.

Mouthereau, F., Deffontaines, B., Lacombe, O. & Angelier, J. 2002. Variations along the strike of the Taiwan thrust belt: basement control on structural style, wedge geometry, and kinematics. *In*: Byrne, T. & Liu, C.S. (eds) *Geology and Geophysics of an Arc–Continent Collision, Taiwan*. Geological Society of America, Special Papers, **358**, 31–54.

Mouthereau, F., Fillon, C. & Ma, K.F. 2009. Distribution of strain rates in the Taiwan orogenic wedge. *Earth and Planetary Science Letters*, **284**, 361–385, http://dx.doi.org/10.1016/j.epsl.2009.05.005.

Murphy, J.B., Waldron, J.W.F., Kontak, D.J., Pe-Piper, G. & Piper, D.J.W. 2011. Minas Fault Zone: late Paleozoic history of an intra-continental orogenic transform fault in the Canadian Appalachians. *Journal of Structural Geology*, **33**, 312–328, http://dx.doi.org/10.1016/j.jsg.2010.11.012.

Narr, W. & Suppe, J. 1994. Kinematics of basement-involved compressive structures. *American Journal of Science*, **294**, 802–860, http://dx.doi.org/10.2475/ajs.294.7.802.

Nicol, A. & Van Dissen, R. 2002. Up-dip partitioning of displacement components on the oblique-slip Clarence Fault, New Zealand. *Journal of Structural Geology*, **24**, 1521–1535, http://dx.doi.org/10.1016/S0191-8141(01)00141-9.

Pérez-Estaún, A., Alvarez-Marrón, J., Brown, D., Puchkov, V., Gorozhanina, Y. & Baryshev, V. 1997. Along-strike structural variations in the foreland thrust and fold belt of the southern Urals. *Tectonophysics*, **276**, 265–280, http://dx.doi.org/10.1016/S0040-1951(97)00060-7.

Rau, R.-J. & Wu, F.T. 1995. Tomographic imaging of lithospheric structures under Taiwan. *Earth and Planetary Science Letters*, **133**, 517–532, http://dx.doi.org/10.1016/0012-821X(95)00076-O.

Rodgers, J. 1987. Chains of basement uplifts within cratons marginal to orogenic belts. *American Journal of Science*, **287**, 661–692, http://dx.doi.org/10.2475/ajs.287.7.661.

Rodriguez-Roa, F.A. & Wiltschko, D.V. 2010. Thrust belt architecture of the central and southern Western Foothills of Taiwan. *In*: Goffey, G.P., Craig, J., Needham, T. & Scott, R. (eds) *Hydrocarbons in Contractional Belts*. Geological Society, London, Special Publications, **348**, 137–168, http://dx.doi.org/10.1144/SP348.8.

Sakaguchi, A., Yanagihara, A., Ujiie, K., Tanaka, H. & Kameyama, M. 2007. Thermal maturity of a fold–thrust belt based on vitrinite reflectance analysis in the Western Foothills complex, western Taiwan. *Tectonophysics*, **443**, 220–232, http://dx.doi.org/10.1016/j.tecto.2007.01.017.

Schmidt, C.J., O'Neill, J.M. & Brandon, W.C. 1988. Influence of Rocky Mountain foreland uplifts on the development of the frontal fold and thrust belt, southwestern Montana. *In*: Schmidt, C.J. & Perry, W.J. (eds) *Interaction of the Rocky Mountain Foreland and the Cordilleran Thrust Belt*. Geological Society of America, Memoirs, **171**, 171–201.

Sibuet, J.-C. & Hsu, S.-K. 2004. How was Taiwan created?. *Tectonophysics*, **379**, 159–181, http://dx.doi.org/10.1016/j.tecto.2003.10.022.

Simoes, M., Avouac, J.P., Beyssac, O., Goffé, B., Farley, K.A. & Chen, Y.-G. 2007. Mountain building in Taiwan: a thermokinematic model. *Journal of Geophysical Research*, **112**, http://dx.doi.org/10.1029/2006JB004824.

Simoes, M., Beyssac, O. & Chen, Y.-G. 2012. Late Cenozoic metamorphism and mountain building in Taiwan: a review. *Journal of Asian Earth Sciences*, **46**, 92–119, http://dx.doi.org/10.1016/j.jseaes.2011.11.009.

Sung, Q., Chen, Y.-C., Tsai, H., Chen, Y.-G. & Chen, W.-S. 2000. Comparison study on the coseismic deformation of the 1999 Chi-Chi earthquake and long-term stream gradient changes along the Chelungpu Fault in central Taiwan. *Terrestrial, Atmospheric and Oceanic Sciences*, **11**, 735–750.

Suppe, J. 1980. A retrodeformable cross section of northern Taiwan. *Proceedings, Geological Society of China*, **23**, 46–55.

Suppe, J. 1981. Mechanics of mountain building and metamorphism in Taiwan. *Memoir of the Geological Society of China*, **4**, 67–89.

Suppe, J. 1984. Kinematics of arc–continent collision, flipping of subduction, and back-arc spreading near Taiwan. *Memoir of the Geological Society of China*, **6**, 21–33.

Suppe, J. 1987. The active Taiwan mountain belt. *In*: Schaer, J.P. & Rodgers, J. (eds) *The Anatomy of Mountain Ranges*. Princeton University Press, Princeton, NJ, 277–293.

Sylvester, A.G. 1988. Strike-slip faults. *Geological Society of America Bulletin*, **100**, 1666– 1703, http://dx.doi.org/10.1130/0016-7606(1988)1002.3.CO;2.

Teng, L.S. & Lin, A.T. 2004. Cenozoic tectonics of the China continental margin: insights from Taiwan. *In*: Malpas, J., Fletcher, C.J.N., Ali, J.R. & Aitchison, J.C. (eds) *Aspects of the Tectonic Evolution of China*. Geological Society, London, Special Publications, **226**, 313–332, http://dx.doi.org/10.1144/GSL.SP.2004.226.01.17.

Teng, L.S., Wang, Y., Tang, C.-H., Huang, C.-Y., Huang, T.-C., Yu, M.-S. & Ke, A. 1991. Tectonic aspects of the Paleogene depositional basin of northern Taiwan. *Proceedings, Geological Society of China*, **34**, 313–336.

Tillman, K.S. & Byrne, T.B. 1995. Kinematic analysis of the Taiwan Slate Belt. *Tectonics*, **14**, 322–341, http://dx.doi.org/10.1029/94TC02451.

Walcott, R.I. 1998. Modes of oblique compression: late Cenozoic tectonics of the South Island of New Zealand. *Reviews of Geophysics*, **36**, 1–26, http://dx.doi.org/10.1029/97RG03084.

Wang, C.-Y., Chang, C.-H. & Yen, H.-Y. 2000. An interpretation of the 1999 Chi-Chi earthquake in Taiwan based on the thin-skinned thrust model. *Terrestrial, Atmospheric and Oceanic Sciences*, **11**, 609–630.

Wang, C.-Y., Li, C.-L., Su, F.-C., Leu, M.-T., Wu, M.-S., Lai, S.-H. & Chern, C.-C. 2002. Structural mapping of the 1999 Chi-Chi earthquake fault, Taiwan by seismic reflection methods. *Terrestrial, Atmospheric and Oceanic Sciences*, **13**, 211–226.

Wilcox, R.E., Harding, T.P. & Seely, D.R. 1973. Basic wrench tectonics. *AAPG Bulletin*, **57**, 74–96.

Wiltschko, D. & Eastman, D. 1983. Role of basement warps and faults in localizing thrust fault ramps. *In*: Hatcher, R.D., Williams, H. & Zietz, I. (eds) *Contributions to the Tectonics and Geophysics of Mountain Chains*. Geological Society of America, Memoirs, **158**, 177–190.

Wiltschko, D., Hassler, L., Hung, J.-H. & Liao, H.-S. 2010. From accretion to collision: motion and evolution of the Chaochou Fault, southern Taiwan. *Tectonics*, **29**, http://dx.doi.org/10.1029/2008TC002398.

Woodward, N.B. 1988. Primary and secondary basement controls on thrust sheet geometries. *In*: Schmidt, C.J. & Perry, W.J. (eds) *Interaction of the Rocky Mountain Foreland and the Cordilleran Thrust Belt*. Geological Society of America, Memoirs, **171**, 353–366.

Wu, F.T., Rau, R.J. & Salzberg, D. 1997. Taiwan orogeny: thin-skinned or lithospheric collision? *Tectonophysics*, **274**, 191–220, http://dx.doi.org/10.1016/S0040-1951(96)00304-6.

Wu, F.T., Chang, C.-H. & Wu, Y.-M. 2004. Precisely relocated hypocentres, focal mechanisms and active orogeny in Central Taiwan. *In*: Malpas, J., Fletcher, C.J.N., Ali, J.R. & Aitchison, J.C. (eds) *Aspects of the Tectonic Evolution of China*. Geological Society, London, Special Publications, **226**, 333–354, http://dx.doi.org/10.1144/gsl.sp.2004.226.01.18.

Wu, Y.-M., Chang, C.-H., Zhao, L., Shyu, J.B.H., Chen, Y.-G., Sieh, K. & Avouac, J.-P. 2007. Seismic tomography of Taiwan: Improved constraints from a dense network of strong motion stations. *Journal of Geophysical Research*, **112**, B08312, http://dx.doi.org/10.1029/2007JB004983.

Wu, Y.-M., Chang, C.-H., Zhao, L., Teng, T.L. & Nakamura, M. 2008*a*. A comprehensive relocation of earthquakes in Taiwan from 1991 to 2005. *Bulletin of the Seismological Society of America*, **98**, 1471–1481, http://dx.doi.org/10.1785/0120070166.

Wu, Y.-M., Zhao, L., Chang, C.-H. & Hsu, Y.-J. 2008*b*. Focal-mechanism determination in Taiwan by genetic algorithm. *Bulletin of the Seismological Society of America*, **98**, 651–661, http://dx.doi.org/10.1785/0120070115.

Wu, Y.-M., Shyu, J.B.H., Chang, C.-H., Zhao, L., Nakamura, M. & Hsu, S.-K. 2009. Improved seismic tomography offshore northeastern Taiwan: Implications for subduction and collision processes between Taiwan and the southernmost Ryukyu. *Geophysical Journal International*, **178**, 1042–1054, http://dx.doi.org/10.1111/j.1365-246X.2009.04180.x.

Wu, Y.-M., Hsu, Y.-J., Chang, C.-H., Teng, L.S.-y & Nakamura, M. 2010. Temporal and spatial variation of stress field in Taiwan from 1991 to 2007: Insights from comprehensive first motion focal mechanism catalog. *Earth and Planetary Science Letters*, **298**, 306–316, http://dx.doi.org/10.1016/j.epsl.2010.07.047.

Yamato, P., Mouthereau, F. & Burov, E. 2009. Taiwan mountain building: Insights from 2-D thermomechanical modelling of a rheologically stratified lithosphere. *Geophysical Journal International*, **176**, 307–326, http://dx.doi.org/10.1111/j.1365-246X.2008.03977.x.

Yanites, B.J., Tucker, G.E., Mueller, K.J., Chen, Y.G., Wilcox, T., Huang, S.Y. & Shi, K.W. 2010. Incision and channel morphology across active structures along the Peikang River, central Taiwan: Implications for the importance of channel width. *Geological Society of America Bulletin*, **122**, 1192–1208, http://dx.doi.org/10.1130/B30035.1.

Yue, L.-F., Suppe, J. & Hung, J.-H. 2005. Structural geology of a classic thrust belt earthquake: the 1999 Chi-Chi earthquake, Taiwan (Mw = 7.6). *Journal of Structural Geology*, **27**, 2058–2083, http://dx.doi.org/10.1016/j.jsg.2005.05.020.

Zoback, M.L. 1992. First- and second-order patterns of stress in the lithosphere: the World Stress Map Project. *Journal of Geophysical Research*, **97**, 11703–11728, http://dx.doi.org/10.1029/92JB00132.

Received 27 February 2013; revised typescript accepted 15 July 2013.
Scientific editing by Quentin Crowley.